

Discrimination Between Healthy Eyes and Those With Mild Glaucoma Damage Using Hemoglobin Measurements of the Optic Nerve Head

Livia Studart de Meneses, MD, Lorena Ribeiro Ciarlini, MD,
Gabriel Ayub, MD, MSc, José Paulo C. Vasconcellos, MD, PhD,
and Vital Paulino Costa, MD, PhD

Précis: The Laguna ONhE, a software that measures the hemoglobin (Hb) concentration of the optic nerve head (ONH) from fundus photographs, demonstrated good accuracy in discriminating healthy eyes from eyes with mild glaucoma.

Purpose: The aim was to evaluate Hb concentration of the optic nerve to distinguish between healthy eyes and eyes with mild glaucoma.

Methods: Eyes from patients with mild primary open angle glaucoma (MD > -6 dB) (n = 58) and from healthy subjects (n = 64) were selected. Retinal nerve fiber layer thickness measurements of all eyes were acquired with optical coherence tomography. Optic disc photographs were also obtained, and the images were analyzed using the Laguna ONhE software, which measures the amount of Hb in 24 sectors of the ONH. The software also calculates the Glaucoma Discriminant Function (GDF), an index that expresses the chance of the ONH being compatible with glaucoma. Areas under the receiver operating characteristic curve and sensitivities at fixed specificities of 90% and 95% of each Laguna ONhE parameter were calculated.

Results: The mean retinal nerve fiber layer thickness and vertical cup/disc ratio of the control and glaucoma groups were $90.0 \pm 10.6 \mu\text{m}$ versus $66.28 \pm 9.85 \mu\text{m}$ ($P < 0.001$) and 0.5 ± 0.09 versus 0.65 ± 0.09 ($P < 0.001$), respectively. Total Hb (67.9 ± 4.45 vs. 62.89 ± 4.89 , $P < 0.001$) and GDF (11.57 ± 15.34 vs. -27.67 ± 20.94 , $P < 0.001$) were significantly higher in the control group. The Hb concentration was also significantly higher in 21 of the 24 sectors in the control group compared with the glaucoma group ($P < 0.05$). The GDF had the largest areas under the receiver operating characteristic curve (0.93), with 79.3% sensitivity at a fixed specificity of 95%.

Conclusion: Measurements of optic nerve Hb concentration using a colorimetry photographic device demonstrated good accuracy in discriminating healthy eyes from eyes with mild glaucoma. Further studies are need to understand vascular factors implicated in the development of glaucoma.

Key Words: glaucoma, diagnosis, OCT, optic nerve, software

(*J Glaucoma* 2022;31:567–573)

Received for publication October 19, 2021; accepted March 17, 2022.
From the Department of Ophthalmology, University of Campinas, Campinas, São Paulo, Brazil.

Disclosure: V.P.C. is a consultant and a member of the speaking bureau for Zeiss, Allergan, Novartis, Alcon, and Iridex. The remaining authors declare no conflict of interest.

Reprints: Livia Studart de Meneses, MD, 251 Vital Brazil Street, Campinas 13083-888, São Paulo, Brazil (e-mail: liviaastudart@gmail.com).

Copyright © 2022 Wolters Kluwer Health, Inc. All rights reserved.
DOI: 10.1097/IJG.0000000000002026

It is estimated that glaucoma, the leading cause of irreversible blindness in the world, affects more than 66 million individuals worldwide, with at least 6.8 million bilaterally blind.¹ Primary open angle glaucoma (POAG) is characterized by a progressive optic neuropathy that leads to changes in the visual field.¹ Early detection of the disease is important, allowing physicians to begin treatment and prevent progression to blindness.²

To diagnose glaucoma, ophthalmologists use a combination of structural and functional manifestations of the disease. In early glaucoma, there is a predominance of structural changes in relation to functional losses.^{3–11} Structural changes can be detected through fundoscopy, retinal scans and, more recently, optical coherence tomography (OCT).^{12–27} OCT offers an accurate analysis of the clinical-structural correlation of glaucomatous damage,²⁸ with high diagnostic accuracy.^{12–26} However, OCT has some limitations related to the presence of artifacts, interference caused by other diseases, as well as age-related changes.^{29–33} In addition, OCT is unavailable in some centers because of the high cost of the device. Furthermore, the impossibility of comparing exams performed by different machines limits the analysis of progression.²⁸ It is necessary, therefore, to seek new methods that are less costly and that show good reproducibility and high diagnostic accuracy.

It has been suggested that changes in blood flow, especially in the concentration of hemoglobin (Hb) in the optic nerve head (ONH), are implicated in the development and progression of glaucoma.^{34–41} The Laguna ONhE software analyzes fundus photographs and is able to determine the limits of the ONH, the cup/disc (C/D) ratio and the Hb concentration throughout the ONH.^{42,43} In addition, the software generates an index (Glaucoma Discriminant Function—GDF), which combines the results of the relative Hb concentrations in various sectors of the ONH and has been shown to have a high diagnostic accuracy.^{34,35,42–48} GDF values range from -100 to +100, and are positive in normal eyes and negative in glaucomatous eyes.⁴⁴

Previous studies have demonstrated that the measurements obtained with the Laguna ONhE software are reproducible.⁴⁷ Furthermore, studies have investigated the sensitivity and specificity of the Laguna ONhE software in populations that included patients with moderate/advanced glaucoma.^{34,35,42–44} However, evaluating the diagnostic accuracy of different technologies in eyes with moderate/advanced glaucoma artificially increases the sensitivity of these methods.⁴⁹ Hence, it is important to verify the diagnostic accuracy of such methods in a population with mild glaucomatous damage. The aim of the present study was to

evaluate the diagnostic accuracy of the Laguna ONhE software in Brazilian patients with mild glaucomatous damage.

METHODS

We conducted a retrospective, case-control study. This study was performed in accordance with the Declaration of Helsinki and was approved by the University of Campinas Medical Institutional Review Board. Since it was based on a review of medical records, the informed consent was waived.

All subjects had undergone a complete ophthalmologic examination, including best corrected visual acuity, slit lamp examination, Goldmann applanation tonometry, gonioscopy, indirect ophthalmoscopy, optic disc evaluation with a 78-diopter lens, color retinography (Canon CR-1 NM Fundus Camera Mark II, Japan) and Spectral-Domain OCT (version 5.1.1.6; Cirrus, Carl Zeiss-Meditec Inc, Dublin, CA). Glaucoma patients also underwent standard achromatic perimetry (SITA 24-2, Humphrey Visual Field Analyzer; Carl Zeiss-Meditec).

To be included in the glaucoma group, all subjects were required to meet the following criteria: (1) previous diagnosis of POAG, defined as the presence of at least 2 of the following optic disc abnormalities: C/D ratio >0.6 , localized loss of neuroretinal tissue, optic disc hemorrhage, or C/D asymmetry >0.3 , (2) mild visual field damage, defined as MD >-6 dB,⁹ (3) open angle on gonioscopy, (4) best corrected visual acuity $\geq 20/40$, (5) refractive error <5 spherical diopters and <3 cylindrical diopters, (6) no history of ocular or systemic disease or surgery that could interfere with colorimetric measurements. Exclusion criteria included: age below 18 years, secondary glaucomas, unreliable visual fields (false positive errors $>15\%$ or fixation losses $>20\%$), low-quality OCTs (quality score <6), and neurological diseases affecting the optic nerve and/or the retina.

Inclusion criteria for the control group were: (1) absence of eye disease, such as age-related macular degeneration, diabetic retinopathy, uveitis and retinal detachment; (2) absence of family history of glaucoma; (3) intraocular pressure <21 mm Hg by Goldmann applanation tonometry; (4) best corrected visual acuity $\geq 20/40$; (5) refractive error <5 spherical diopters and <3 cylindrical diopters; (6) open angle on gonioscopy; and (7) normal appearance of the optic disc based on stereoscopic clinical examination. An OCT showing peripapillary retinal nerve fiber layer thickness (RNFLT) measurements (average thickness) within normal limits and no evidence of localized RNFL defect was also required. Exclusion criteria for the control group were (1) age below 18 years; (2) optic disc abnormalities compatible with glaucoma, as described above; (3) OCT abnormalities compatible with glaucomatous damage; (4) OCT image with quality score <6 ; (5) neurological diseases affecting the optic nerve and/or retina. One eye from each subject was randomly chosen to enter the study. Color photographic images were obtained by trained examiners, using a Canon CR-1 nonmydriatic fundus retinograph (Canon CR-1 NM Fundus Camera Mark II; Japan). Retinography images were incorporated into the Laguna ONhE software by 1 examiner, and the following parameters were measured: Hb concentration (total and in the 24 ONH sectors), C/D ratio and GDF.

Laguna ONhE analyzes three spectral components of ONH photographs: blue (B), green (G), and red (R). The

ONH areas with high Hb content mainly reflect red light. In contrast, areas with a low Hb content reflect a lower proportion of the red component compared with the green and blue light. A previous experimental study has demonstrated that the photographic images obtained with this technique can be used to determine the amount of Hb in the tissue.³⁵ The value of the equation obtained in the tissue area is divided by the value obtained in the vessels and this result is multiplied by 100, thus obtaining the Hb concentration in the tissue.⁴²

With the application of image segmentation methods based on color patterns and identification of components compatible with the shape of the ONH, it is possible to automatically determine its limits.³⁵ The C/D ratio estimation is automatically performed in all cases. Similarly, the program performs an automatic delimitation of the central retinal artery, central retinal vein and their main branches to use as a reference value for Hb concentration. Subsequently, the program builds a map displaying the Hb concentration in each sector of the ONH, using a color scale that identifies the amount of Hb: warmer colors represent high Hb concentration and cooler colors represent areas of less perfusion and thinner tissue³⁵ (Fig. 1).

To calculate the GDF index and the C/D ratio, the program divides the ONH into 3 concentric rings and each ring is divided into 8 sectors (total = 24 sectors) (Fig. 1). The outer ring lines up with the neuroretinal rim, the middle ring corresponds to a transitional area, which may include both the neuroretinal rim and the cup, and the inner border mainly comprises the cup.

The statistical analysis was performed with the Statistical Package for Social Sciences—SPSS (version 22.0; IBM Corporation, Armonk, NY). Normality was assessed by the Shapiro-Wilk test. Categorical variables were compared between the 2 groups using the χ^2 test or the Fisher exact test, whereas continuous variables were compared using the 1-tailed unpaired *t* test or the Mann-Whitney *U* test. Receiver operating characteristic curves were built, and areas under the curve (AUC), sensitivities and specificities at fixed specificities of 90% and 95%, were calculated for each Laguna ONhE parameter with MedCalc (version 19.3.1; MedCalc Software Ltd, Ostend, Belgium). The log-rank test was used to compare AUCs obtained with different parameters.⁵⁰ *P*-values <0.05 were considered statistically significant. We used the Bonferroni correction when multiple comparisons were performed.

RESULTS

One hundred and thirty eyes were found to be eligible, and 122 were included in the analysis. Eight eyes (6.15%) were excluded because retinal images could not be evaluated by the Laguna ONhE software. The control group included 64 eyes and the glaucoma group included 58 eyes. The mean MD in the glaucoma group was -2.85 ± 1.9 dB, and 8 eyes (13.8%) had preperimetric glaucoma. Baseline characteristics of both groups are listed in Table 1.

There were no differences in age, sex, and race distributions between the glaucoma and control groups ($P > 0.05$). As expected, the glaucoma group had a thinner RNFLT (66.28 ± 9.85 vs. 90 ± 10.6 μm , $P < 0.0001$). Table 2 displays the Laguna ONhE parameters obtained in both groups. The glaucoma group had larger vertical cup/disc ratios (0.65 ± 0.09 vs. 0.5 ± 0.09 , $P < 0.0001$) and cup/disc ratios area (0.44 ± 0.12 vs. 0.29 ± 0.1 , $P < 0.0001$) than

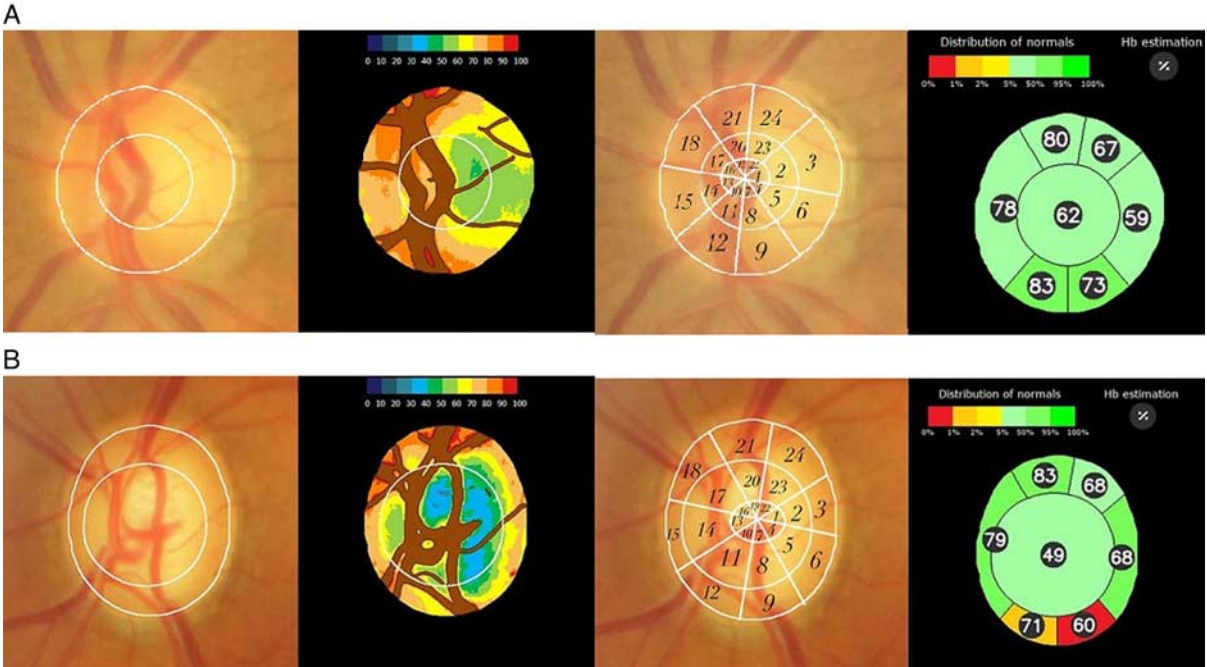


FIGURE 1. Example of Laguna ONHe analysis of a normal eye (A) and 1 eye with early glaucoma (B) with estimation of the optic disc cup from Hb distribution and segmentation of reference vessels and pseudocolor image of Hb distribution. Sector areas are compared with the reference value of the central vessels, which represent 100% of Hb, and thus the percentage of Hb in each sector is obtained. The software Laguna ONHe uses a photographic image of the optic nerve head, divided into 24 sectors to estimate Hb in each sector and 3 concentric rings. HB indicates hemoglobin. Figure 1 can be viewed in color online at www.glaucomajournal.com.

the control group. Mean total Hb concentration was significantly lower in the glaucoma group ($67.9 \pm 4.45\%$ vs. $62.89 \pm 4.89\%$, $P < 0.0001$). Also, mean Hb concentrations in all sectors were lower in the glaucoma group, although the differences were not statistically significant in sectors 2, 3, 6, 12–15, 18, 21, and 24 ($P > 0.002$ following Bonferroni correction). Mean GDF was significantly higher in the control group (11.57 ± 15.34 vs. -27.67 ± 20.94 , $P < 0.0001$) (Table 2).

Table 3 displays the AUCs, and the sensitivities at fixed specificities of 90% and 95% of all parameters. GDF obtained the largest AUC (0.93), and the best sensitivities at 90% (82.76%) and 95% (79.31%) specificities. Hb in Sector 8

(AUC = 0.888) and Hb total (AUC = 0.804) also showed good diagnostic accuracy. The AUC obtained with GDF was significantly larger than those obtained with Hb Total ($P = 0.001$) and Hb Cup ($P < 0.001$). The AUC obtained with Hb in Sector 8 was also significantly larger than those obtained with Hb total ($P = 0.006$) and Hb cup ($P < 0.001$). There was no statistically significant difference between the AUCs obtained with GDF and Hb sector 8 ($P = 0.154$) (Fig. 2).

DISCUSSION

Clinical evaluation and documentation of the ONH are essential for the diagnosis and monitoring of glaucoma.¹ Optic disc photographs can be used to monitor eyes that are suspicious or have a diagnosis of glaucoma.¹ However, its interpretation is subjective and shows great intraobserver and interobserver variabilities.^{51–57} Computerized imaging exams have emerged as an objective way to provide quantitative measurements of the ONH and RNFL, assisting ophthalmologists in the diagnosis and follow-up of glaucoma.⁵¹ As mentioned before, OCT offers high reproducibility and high accuracy for the diagnosis of glaucoma and has been widely used in clinical care.^{12–27} However, it is an expensive tool, with prices varying between USD 40,000 and USD 150,000⁵⁸ which may limit its use in unprivileged environments. Our study shows that Laguna ONHe, an accessible and easy-to-use technology (at a cost of USD 1 per image analyzed, www.retinalyze.com) which requires only a fundus camera to obtain the images and a software that determines the amount of Hb in the ONH, provides high sensitivity and specificity for the diagnosis of early glaucoma.

TABLE 1. Baseline Characteristics of Both Groups

	Control Group (n = 64)	Glaucoma Group (n = 58)	P
Sex (male/female)	36/28	31/27	0.756†
Age (y)	60.47 ± 14.55	62.16 ± 14.29	0.339†
Race (European descent/ Asian descent)	64/0	55/3	0.105‡
Laterality (right/left)	31/33	30/28	0.717§
MD (dB)	—	−2.85 ± 1.9	—
RNFLT (μm)	90 ± 10.6	66.28 ± 9.85	< 0.001*

Statistically significant *P*-values are in bold.

*One-tailed nonpaired *t* test.

†Mann-Whitney *U* test.

‡Fisher exact test.

§ χ^2 test.

RNFLT indicates retinal nerve fiber layer thickness.

TABLE 2. Mean GDF, CDR, CD Area, and Mean Hb Concentrations in Each Sector in the Control and Glaucoma Groups

	Control	Glaucoma	P
GDF	11.57 ± 15.34	−27.67 ± 20.94	< 0.0001†
Vertical CDR	0.5 ± 0.09	0.65 ± 0.09	< 0.0001†
CD area	0.29 ± 0.1	0.44 ± 0.12	< 0.0001†
Hb total	67.9 ± 4.45	62.89 ± 4.89	< 0.0001†
Hb cup	58.67 ± 9.72	52.68 ± 7.72	< 0.0001†
Hb Sector 1	71.63 ± 11.76	58.46 ± 13.61	< 0.0001†
Hb Sector 2	76.69 ± 4.6	74.70 ± 7.42	0.0403*
Hb Sector 3	77.53 ± 3.69	78.62 ± 4.72	0.0785*
Hb Sector 4	69.97 ± 11.57	56.63 ± 13.03	< 0.0001†
Hb Sector 5	77.78 ± 3.83	70.88 ± 7.16	< 0.0001*
Hb Sector 6	79.33 ± 3.64	79.3 ± 3.73	0.854†
Hb Sector 7	61.38 ± 10.77	49.55 ± 11.06	< 0.0001*
Hb Sector 8	72.38 ± 5.46	59.19 ± 9.15	< 0.0001†
Hb Sector 9	78.21 ± 4.0	73.74 ± 7.1	< 0.0001†
Hb Sector 10	51.78 ± 10.62	44.66 ± 9.28	0.0001*
Hb Sector 11	59.15 ± 7.27	51.67 ± 7.93	< 0.0001*
Hb Sector 12	63.84 ± 4.08	61.81 ± 4.92	0.0075*
Hb Sector 13	48.45 ± 11.04	43.26 ± 8.43	0.002*
Hb Sector 14	53.46 ± 7.58	50.29 ± 7.48	0.0108*
Hb Sector 15	57.06 ± 4.46	58.92 ± 5.32	0.0195*
Hb Sector 16	52.19 ± 11.51	45.83 ± 9.46	0.0005*
Hb Sector 17	62.17 ± 7.58	54.92 ± 9.58	< 0.0001†
Hb Sector 18	66.65 ± 3.92	67.6 ± 5.33	0.375†
Hb Sector 19	61.28 ± 13.3	51.29 ± 13.15	0.0001*
Hb Sector 20	75.43 ± 9.28	64.62 ± 12.32	< 0.0001†
Hb Sector 21	81.26 ± 4.65	79.45 ± 4.92	0.0195*
Hb Sector 22	69.49 ± 14.07	56.96 ± 14.37	< 0.0001†
Hb Sector 23	81.6 ± 9.07	74.49 ± 10.76	< 0.0001†
Hb Sector 24	83.58 ± 4.62	82.68 ± 4.61	0.1418*

Statistically significant *P*-values (*P* < 0.002) following the Bonferroni correction, are in bold.

*One-tailed unpaired *t* test.

†Mann-Whitney *U* test.

CD indicates cup/disc; CDR, cup/disc ratios; GDF, Glaucoma Discriminant Function; Hb, hemoglobin.

TABLE 3. AUCs and Sensitivities at Fixed Specificities of 90% and 95% of Laguna ONHe Parameters

	AUC	Sensitivity at Fixed 90% Specificity	Sensitivity at Fixed 95% Specificity
GDF	0.93	82.76	79.31
Vertical CDR	0.887	76.56	56.25
CD Area	0.848	73.44	42.19
Hb total	0.804	56.9	48.28
Hb cup	0.704	29.31	10.34
Hb Sector 1	0.781	53.45	70.34
Hb Sector 2	0.576	34.48	18.97
Hb Sector 3	0.582	18.97	17.24
Hb Sector 4	0.79	58.62	24.14
Hb Sector 5	0.805	60.34	55.17
Hb Sector 6	0.51	12.07	3.45
Hb Sector 7	0.788	43.1	34.48
Hb Sector 8	0.888	81.03	75.86
Hb Sector 9	0.695	44.83	31.03
Hb Sector 10	0.693	24.14	17.24
Hb Sector 11	0.76	27.59	22.41
Hb Sector 12	0.623	27.59	18.97
Hb Sector 13	0.635	15.52	12.07
Hb Sector 14	0.612	18.97	12.07
Hb Sector 15	0.595	25.86	20.69
Hb Sector 16	0.661	24.14	15.62
Hb Sector 17	0.73	46.55	41.38
Hb Sector 18	0.547	25.86	15.52
Hb Sector 19	0.715	44.83	25.86
Hb Sector 20	0.772	48.28	46.55
Hb Sector 21	0.612	17.24	8.62
Hb Sector 22	0.748	36.21	27.59
Hb Sector 23	0.728	46.55	31.03
Hb Sector 24	0.575	8.62	3.45

AUC indicates area under the curve; CD, cup/disc; CDR, cup/disc ratios; GDF, Glaucoma Discriminant Function; Hb, hemoglobin.

Optic nerve ischemia and reduced ocular blood flow have been suggested to participate in the development and progression of glaucomatous damage.^{59–61} Optic nerve perfusion depends on 3 factors: oxygen saturation, blood flow, and amount of Hb. It has been advocated that changes in ONH reflectance can detect variations in Hb levels, indirectly measuring ONH perfusion.^{35,62} Previous studies have investigated the diagnostic accuracy of the Laguna ONHe software.^{35,46} Although comparisons between the various published studies investigating the diagnostic ability of the Laguna ONHe software are hampered by demographic differences, diverse inclusion and exclusion criteria, and by different levels of severity of damage, their results are listed below.⁶³

de la Rosa et al³⁵ evaluated the diagnostic accuracy of the Laguna ONHe software in 102 healthy individuals and 101 patients with moderate glaucomatous damage (MD = −9.30 ± 9.3 dB). The authors reported that the GDF had an AUC of 0.97, with 89% sensitivity at a fixed specificity of 95%. Mendez-Hernandez et al⁴⁶ compared the diagnostic ability of Laguna ONHe with OCT and confocal scanning laser ophthalmoscopy (HRT III). Sixty six POAG patients and 52 healthy eyes underwent measurements with the Spectralis OCT, HRT III, and Laguna ONHe. Among the 66 POAG patients, 32 had mild, 19 had moderate, and 15 had advanced glaucomatous damage (mean MD = −7.74 dB). The AUCs were 0.785 (95% CI: 0.700–0.863) for GDF, 0.807 (95% CI: 0.730–0.883) for OCT RNFLT and 0.714

(95% CI: 0.618–0.810) and 0.721 (95% CI: 0.628–0.815) for the HRT III GPS (glaucoma probability score) and the HRT III vertical C/D ratio, respectively. The authors concluded that the diagnostic accuracy of Laguna ONHe was similar to those obtained with OCT and HRT III.

In another paper, Mendez-Hernandez et al⁶⁴ evaluated the performance of the Laguna ONHe software in 67 POAG patients and 41 controls. Mean MD in POAG patients was −4.57 dB, but there is no description of the number of patients with mild, moderate or advanced glaucoma. The AUC obtained with the GDF parameter was 0.92, with a 75% sensitivity at 95% specificity. Pena-Betancor et al⁴² analyzed 87 healthy eyes 71 and glaucoma eyes with the Laguna ONHe software. Glaucomatous eyes had a mean MD of −10.53 ± 9.02 dB, indicating that most had moderate to advanced glaucomatous damage. The GDF parameter showed an AUC of 0.896 (95% CI: 0.84–0.95), with 67% sensitivity at a fixed specificity of 95%.

It is noteworthy that the above-mentioned studies did not exclude patients with moderate or severe glaucomas, which tends to increase the diagnostic accuracy of the tested method. Our study is the first one to investigate the diagnostic accuracy of Laguna ONHe exclusively in eyes with early glaucomatous damage (MD > −6dB). We identified the GDF index as the best diagnostic parameter, associated with a large AUC (0.93), and a high sensitivity (79.3%) at a fixed specificity of 95%. Interestingly, the AUC obtained in this study with the GDF is comparable to those reported in

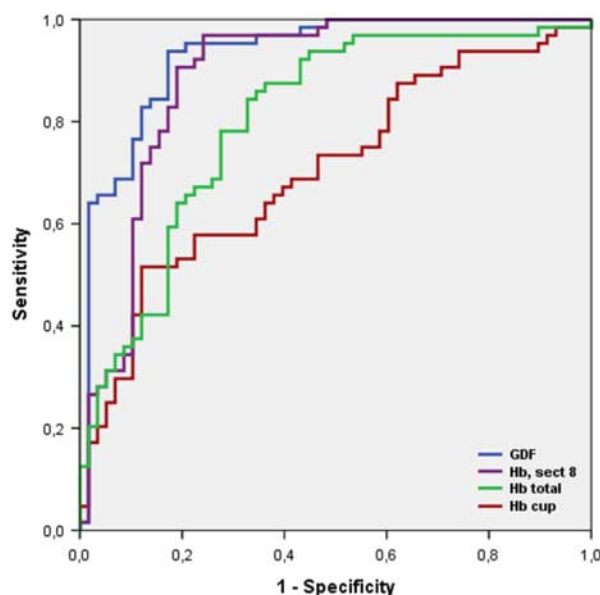


FIGURE 2. Receiver operating characteristic curves of some diagnostic parameters of the Laguna ONhE software: GDF, Hb sector 8, Hb total, and Hb cup. GDF indicates Glaucoma Discriminant Function; Hb, hemoglobin. Figure 2 can be viewed in color online at www.glaucomajournal.com.

series including patients with moderate and advanced glaucoma. Furthermore, the AUC reported herein is comparable to those reported with OCT measurements in eyes with early glaucoma, which varied between 0.844 and 0.92.^{65–69} The Hb concentration at sector 8, localized in the inferior ONH rim, was also associated with good diagnostic accuracy (AUC = 0.888). This finding is in accordance with other reports that have indicated that the inferior sectors of the optic nerve and RNFL appear to be affected earlier in glaucoma, with better diagnostic performances than other sectors.^{70,71}

The limitations of this study include those that apply to any retrospective study, including selection bias and the fact that it was conducted in a single center with a relative small sample size. In addition, as in all imaging methods, the Laguna ONhE software is also affected by artifacts. In fact, some retinal scans (6.5%) could not be read by the software, indicating that some photographs may not have enough quality to be analyzed by Laguna ONhE. In fact, the reported proportions of eyes that could not be analyzed in other series varied from 1.3% to 12%.^{34,35,42,47} Finally, because this is cross-sectional study, with a selection of cases with well-established glaucoma and clearly normal individuals, the diagnostic accuracy obtained may be overestimated. It would have been preferable to evaluate the performance of the Laguna ONhE software in suspicious patients followed longitudinally to determine those who would progress to glaucoma.

In conclusion, our results suggest that the Laguna ONhE software, an accessible method to diagnose glaucoma based on fundus photographs, shows good diagnostic accuracy to differentiate normal eyes from eyes with mild glaucoma. Longitudinal studies with a larger number of patients are necessary to confirm our findings and to evaluate if this technology can be used in the follow-up of glaucoma patients.

REFERENCES

- Weinreb RN, Tee Khaw P. Primary open-angle glaucoma. *Lancet*. 2004;36:1711–1720.
- Peters D, Bengtsson B, Heijl A. Factors associated with lifetime risk of open-angle glaucoma blindness. *Acta Ophthalmol*. 2014; 92:421–425.
- Medeiros FA, Alencar LM, Zangwill LM, et al. Prediction of functional loss in glaucoma from progressive optic disc damage. *Arch Ophthalmol*. 2009;127:1250–1256.
- Hood DC, Kardon RH. A framework for comparing structural and functional measures of glaucomatous damage. *Prog Retin Eye Res*. 2007;26:688–710.
- Harwerth RS, Carter-Dawson L, Smith EL, et al. Neural losses correlated with visual losses in clinical perimetry. *Investig Ophthalmol Vis Sci*. 2004;45:3152–3160.
- Kass MA, Heuer DK, Higginbotham EJ, et al. The ocular hypertension treatment study. *Arch Ophthalmol*. 2002;120: 701–713.
- The European Glaucoma Prevention Study (EGPS) Group. Results of the European Glaucoma Prevention Study. *Ophthalmology*. 2005;112:366–375.
- Wollstein G, Schuman JS, Price LL, et al. Optical coherence tomography longitudinal evaluation of retinal nerve fiber layer thickness in glaucoma. *Arch Ophthalmol*. 2005;123:464–470.
- Strouthidis NG, Scott A, Peter NM, et al. Optic disc and visual field progression in ocular hypertensive subjects: detection rates, specificity, and agreement. *Investig Ophthalmol Vis Sci*. 2006;47:2904–2910.
- Leung CKS, Cheung CYL, Weinreb RN, et al. Evaluation of retinal nerve fiber layer progression in glaucoma: a study on optical coherence tomography guided progression analysis. *Investig Ophthalmol Vis Sci*. 2010;51:217–222.
- Medeiros FA, Alencar LM, Zangwill LM, et al. The relationship between intraocular pressure and progressive retinal nerve fiber layer loss in glaucoma. *Ophthalmology*. 2009;116:1125–1133.
- Medeiros FA, Zangwill LM, Bowd C, et al. Influence of disease severity and optic disc size on the diagnostic performance of imaging instruments in glaucoma. *Investig Ophthalmol Vis Sci*. 2006;47:1008–1015.
- Schuman JS, Pedut-Kloizman T, Hertzmark E, et al. Reproducibility of nerve fiber layer thickness measurements using optical coherence tomography. *Ophthalmology*. 1996;103:1889–1898.
- Schuman JS, Hee MR, Puliafito CA, et al. Quantification of nerve fiber layer thickness in normal and glaucomatous eyes using optical coherence tomography: a pilot study. *Arch Ophthalmol*. 1995;113:586–596.
- Bowd C, Weinreb RN, Williams JM, et al. The retinal nerve fiber layer thickness in ocular hypertensive, normal, and glaucomatous eyes with optical coherence tomography. *Arch Ophthalmol*. 2000;118:22–26.
- Zangwill LM, Bowd C, Berry CC, et al. Discriminating between normal and glaucomatous eyes using the Heidelberg Retina Tomograph, GDx Nerve Fiber Analyzer, and Optical Coherence Tomograph. *Arch Ophthalmol*. 2001;119:985–993.
- Williams ZY, Schuman JS, Gamell L, et al. Optical coherence tomography measurement of nerve fiber layer thickness and the likelihood of a visual field defect. *Am J Ophthalmol*. 2002;134: 538–546.
- Bowd C, Zangwill LM, Berry CC, et al. Detecting early glaucoma by assessment of retinal nerve fiber layer thickness and visual function. *Investig Ophthalmol Vis Sci*. 2001;42:1993–2003.
- Budenz DL, Fredette MJ, Feuer WJ, et al. Reproducibility of peripapillary retinal nerve fiber thickness measurements with stratus OCT in glaucomatous eyes. *Ophthalmology*. 2008;115: 661–666.
- Paunescu LA, Schuman JS, Price LL, et al. Reproducibility of nerve fiber thickness, macular thickness, and optic nerve head measurements using StratusOCT. *Investig Ophthalmol Vis Sci*. 2004;45:1716–1724.
- Gürses-Özden R, Teng C, Vessani R, et al. Macular and retinal nerve fiber layer thickness measurement reproducibility using

- optical coherence tomography (OCT-3). *J Glaucoma*. 2004;13:238–244.
22. DeLeón Ortega JE, Sakata LM, Kakati B, et al. Effect of glaucomatous damage on repeatability of confocal scanning laser ophthalmoscope, scanning laser polarimetry, and optical coherence tomography. *Investig Ophthalmol Vis Sci*. 2007;48:1156–1163.
 23. Blumenthal EZ, Williams JM, Weinreb RN, et al. Reproducibility of nerve fiber layer thickness measurements by use of optical coherence tomography. *Ophthalmology*. 2000;107:2278–2282.
 24. Medeiros FA, Zangwill LM, Bowd C, et al. Comparison of the GDx VCC scanning laser polarimeter, HRT II confocal scanning laser ophthalmoscope, and stratus OCT optical coherence tomograph for the detection of glaucoma. *Arch Ophthalmol*. 2004;122:827–837.
 25. Lu ATH, Wang M, Varma R, et al. Combining nerve fiber layer parameters to optimize glaucoma diagnosis with optical coherence tomography. *Ophthalmology*. 2008;115:5–7.
 26. Huang D, Swanson EA, Lin CP, et al. Optical coherence tomography. *Science*. 1991;254:1178–1181.
 27. Jampel HD, Friedman D, Quigley H, et al. Agreement among glaucoma specialists in assessing progressive disc changes from photographs in open-angle glaucoma patients. *Am J Ophthalmol*. 2009;147:39–44.
 28. Vessani RM, Gracitelli CPB, Leite M. Diretrizes para utilização do OCT para glaucoma. *Soc Bras Glaucoma*. 2019;1:1–15.
 29. Han IC, Jaffe GJ. Evaluation of artifacts associated with macular spectral-domain optical coherence tomography. *Ophthalmology*. 2010;117:1177–1189.
 30. Somfai GM, Salinas HM, Puliafito CA, et al. Evaluation of potential image acquisition pitfalls during optical coherence tomography and their influence on retinal image segmentation. *J Biomed Opt*. 2007;12:041209.
 31. Melo GB, Libera RD, Barbosa AS, et al. Comparison of optic disk and retinal nerve fiber layer thickness in nonglaucomatous and glaucomatous patients with high myopia. *Am J Ophthalmol*. 2006;142:858–860.
 32. Arintawati P, Sone T, Akita T, et al. The applicability of ganglion cell complex parameters determined from SD-OCT images to detect glaucomatous eyes. *J Glaucoma*. 2013;22:713–718.
 33. Song AP, Wu XY, Wang JR, et al. Measurement of retinal thickness in macular region of high myopic eyes using spectral domain OCT. *Int J Ophthalmol*. 2013;7:122–127.
 34. Medina-Mesa E, Gonzalez-Hernandez M, Sigut J, et al. Estimating the amount of hemoglobin in the neuroretinal rim using color images and OCT. *Curr Eye Res*. 2016;41:798–805.
 35. de la Rosa MG, Gonzalez-Hernandez M, Sigut J, et al. Measuring hemoglobin levels in the optic nerve head: comparisons with other structural and functional parameters of glaucoma. *Investig Ophthalmol Vis Sci*. 2013;54:482–489.
 36. Gonzalez-Hernandez M, Gonzalez-Hernandez D, Perez-Barbudo D, et al. Fully automated colorimetric analysis of the optic nerve aided by deep learning and its association with perimetry and OCT for the study of glaucoma. *J Clin Med*. 2021;10:3231.
 37. Jia Y, Morrison JC, Tokayer J, et al. Quantitative OCT angiography of optic nerve head blood flow. *Biomed Opt Express*. 2012;3:183–189.
 38. Petrig BL, Riva CE, Hayreh SS. Laser Doppler flowmetry and optic nerve head blood flow. *Am J Ophthalmol*. 1999;127:413–425.
 39. Hayreh SS. Blood supply of the optic nerve head and its role in optic atrophy, glaucoma, and oedema of the optic disc. *Br J Ophthalmol*. 1969;53:721–748.
 40. Hayreh SS. Progress in the understanding of the vascular etiology of glaucoma. *Curr Opin Ophthalmol*. 1994;5:26–35.
 41. Hayreh SS. Posterior ciliary artery circulation in health and disease the weissenfeld lecture. *Invest Ophthalmol Vis Sci*. 2004;45:749–757.
 42. Pena-Betancor C, Gonzalez-Hernandez M, Fumero-Batista F, et al. Estimation of the relative amount of hemoglobin in the cup and neuroretinal rim using stereoscopic color fundus images. *Investig Ophthalmol Vis Sci*. 2015;56:1562–1568.
 43. Gonzalez-Hernandez M, Saavedra JS, De La Rosa MG. Relationship between retinal nerve fiber layer thickness and hemoglobin present in the optic nerve head in glaucoma. *J Ophthalmol*. 2017;2017:2–8.
 44. De La Rosa MG. Measuring hemoglobin levels in the optic nerve head for glaucoma management. *Glaucoma Imaging*. 2016;54:265–279.
 45. Rodriguez Uña I, Méndez Hernández CD, Sáenz-Francés F, et al. Correlating cup-to-disc ratios measured by HRT-III, SD-OCT and the new color imaging Laguna ONhE procedure. *Arch Soc Esp Oftalmol*. 2015;90:212–219.
 46. Mendez-Hernandez C, Rodriguez-Uña I, De La Rosa MG, et al. Glaucoma diagnostic capacity of optic nerve head haemoglobin measures compared with spectral domain OCT and HRT III confocal tomography. *Acta Ophthalmol*. 2016;94:697–704.
 47. Mendez-Hernandez C, Garcia-Feijoo J, Arribas-Pardo P, et al. Reproducibility of optic nerve head hemoglobin measures. *J Glaucoma*. 2016;25:348–354.
 48. Peruch-González L, Méndez-Hernández CD, De La Rosa MG, et al. Preliminary study of the differences in optic nerve head hemoglobin measures between patients with and without childhood glaucoma. *J Pediatr Ophthalmol Strabismus*. 2017;54:387–394.
 49. Silva FR, Vidotti VG, Cremasco F, et al. Sensitivity and specificity of machine learning classifiers for glaucoma diagnosis using spectral domain oct and standard automated perimetry. *Arq Bras Oftalmol*. 2013;76:170–174.
 50. Zhou XH, Obuchowski NA, McClish DK. *Statistical Methods in Diagnostic Medicine*. New York, NY: Wiley-Interscience; 2002.
 51. Reus NJ, De Graaf M, Lemij HG. Accuracy of GDx VCC, HRT I, and clinical assessment of stereoscopic optic nerve head photographs for diagnosing glaucoma. *Br J Ophthalmol*. 2007;91:313–318.
 52. Breusegem C, Fieuws S, Stalmans I, et al. Agreement and accuracy of non-expert ophthalmologists in assessing glaucomatous changes in serial stereo optic disc photographs. *Ophthalmology*. 2011;118:742–746.
 53. Varma R, Steinmann WC, Scott IU. Expert agreement in evaluating the optic disc for glaucoma. *Ophthalmology*. 1992;99:215–221.
 54. Abrams LS, Scott IU, Spaeth GL, et al. Agreement among optometrists, ophthalmologists, and residents in evaluating the optic disc for glaucoma. *Ophthalmology*. 1994;101:1662–1667.
 55. Greaney MJ, Hoffman DC, Garway-Heath DF, et al. Comparison of optic nerve imaging methods to distinguish normal eyes from those with glaucoma. *Investig Ophthalmol Vis Sci*. 2002;43:140–145.
 56. Wollstein G, Garway-Heath DF, Fontana L, et al. Identifying early glaucomatous changes: comparison between expert clinical assessment of optic disc photographs and confocal scanning ophthalmoscopy. *Ophthalmology*. 2000;107:2272–2277.
 57. Girkin CA, McGwin G, Long C, et al. Subjective and objective optic nerve assessment in African Americans and whites. *Investig Ophthalmol Vis Sci*. 2004;45:2272–2278.
 58. Olson J, Sharp P, Goatman K, et al. Improving the economic value of photographic screening for optical coherence tomography-detectable macular oedema: a prospective, multicentre, UK study. *Health Technol Assess*. 2013;17:1–142.
 59. Schmidl D, Garhofer G, Schmetterer L. The complex interaction between ocular perfusion pressure and ocular blood flow—relevance for glaucoma. *Exp Eye Res*. 2011;93:141–155.
 60. Moore NA, Harris A, Wentz S, et al. Baseline retrolubar blood flow is associated with both functional and structural glaucomatous progression after 4 years. *Br J Ophthalmol*. 2017;101:305–308.
 61. Park HYL, Kim JW, Park CK. Choroidal microvasculature dropout is associated with progressive retinal nerve fiber layer thinning in glaucoma with disc hemorrhage. *Ophthalmology*. 2018;125:1003–1013.

62. Crittin M, Riva CE. Functional imaging of the human papilla and peripapillary region based on flicker-induced reflectance changes. *Neurosci Lett*. 2004;360:141–144.
63. Barella KA, Costa VP, Vidotti VG, et al. Glaucoma diagnostic accuracy of machine learning classifiers using retinal nerve fiber layer and optic nerve data from SD-OCT. *J Ophthalmol*. 2013;2013:3.
64. Mendez-Hernandez C, Wang S, Arribas-Pardo P, et al. Diagnostic validity of optic nerve head colorimetric assessment and optical coherence tomography angiography in patients with glaucoma. *Br J Ophthalmol*. 2021;105:957–963.
65. Gonzalez-Hernandez D. Segmentation of the optic nerve head based on deep learning to determine its hemoglobin content in normal and glaucomatous subjects. *J Clin Exp Ophthalmol*. 2018;9:5–7.
66. Raza AS, Zhang X, De Moraes CGV, et al. Improving glaucoma detection using spatially correspondent clusters of damage and by combining standard automated perimetry and optical coherence tomography. *Investig Ophthalmol Vis Sci*. 2014;55:612–624.
67. Medeiros FA, Lisboa R, Weinreb RN, et al. A combined index of structure and function for staging glaucomatous damage. *Arch Ophthalmol*. 2012;130:1107–1116.
68. Vessani RM, Moritz R, Batis L, et al. Comparison of quantitative imaging devices and subjective optic nerve head assessment by general ophthalmologists to differentiate normal from glaucomatous eyes. *J Glaucoma*. 2009;18:253–261.
69. DeLeón-Ortega JE, Arthur SN, McGwin G, et al. Discrimination between glaucomatous and nonglaucomatous eyes using quantitative imaging devices and subjective optic nerve head assessment. *Investig Ophthalmol Vis Sci*. 2006;47:3374–3380.
70. Amini N, Nowroozizadeh S, Cirineo N, et al. Influence of the disc-fovea angle on limits of RNFL variability and glaucoma discrimination. *Invest Ophthalmol Vis Sci*. 2014;55:7332–7342.
71. Lee WJ, Kyeong IN, Kim YK, et al. Diagnostic ability of wide-field retinal nerve fiber layer maps using swept-source optical coherence tomography for detection of preperimetric and early perimetric glaucoma. *J Glaucoma*. 2017;26:577–585.